Title
APPROXIMATE METHODS FOR CALCULATION OF INTRINSIC TOTAL-ABSORPTION-AND DOUBLE-ESCAPE-PEAK EFFICIENCIES FOR Ge(Li) DETECTORS

Authors
Euler, B.A.
Kaplan, S.N.

Publication Date
1969-10-01

For IEEE Nuclear Science Symposium,
San Francisco, Ca., October 29-31, 1969

UCRL-19392
Preprint

c. 2

APPROXIMATE METHODS FOR CALCULATION OF INTRINSIC TOTAL-ABSORPTION- AND DOUBLE-ESCAPE-PEAK EFFICIENCIES FOR Ge(Li) DETECTORS

B. A. Euler and S. N. Kaplan

October 1969

AEC Contract No. W-7405-eng-48

LAWRENCE RADIATION LABORATORY
UNIVERSITY of CALIFORNIA BERKELEY

APPROXIMATE METHODS FOR CALCULATION OF INTRINSIC TOTAL-ABSORPTION- AND DOUBLE-ESCAPE-PEAK EFFICIENCIES FOR Ge(Li) DETECTORS

B. A. Euler*
Department of Nuclear Engineering
University of California
Berkeley, California

S. N. Kaplan
Department of Nuclear Engineering
and
Lawrence Radiation Laboratory†
University of California
Berkeley, California

Abstract

Approximate methods are presented for calculation of intrinsic total-absorption- and double-escape-peak efficiencies of Ge(Li) detectors. These methods utilize "average" characteristics of gamma-ray photon interactions with matter, and, while developed in this paper for specific application to the Ge(Li) detector efficiency problem, should be applicable to any gamma-ray detector or absorptive medium. The technique for total-absorption-peak efficiency determination includes the use of an "average-photon energy-degradation curve" and of the Dirac chord method for calculation of collision probabilities. The average-photon energy-degradation curve is obtained from differential Compton collision cross sections and detector material total-cross-section characteristics; it is independent of detector size and shape. The Dirac chord method is then used to determine the probability of further collisions for photons "generated" within the detector volume. In the model these probabilities are functions only of a characteristic detectors dimension, $\bar{s}\mu$, where $\bar{s}$ is the average chord length and μ is the total linear attenuation coefficient. Double-escape-peak efficiencies are determined through the calculation of the average probability of occurrence of the following three phenomena: (1) pair production, (2) electron-positron absorption, and (3) annihilation-photon double escape. Complete working curves and expressions are included to enable convenient utilization of these techniques. Example results are compared with efficiency determinations made experimentally and by Monte Carlo calculations.

Introduction

The use of Ge(Li) detectors is becoming increasingly widespread, not only for nuclear spectroscopy studies, but also as an analytical tool for material analysis. In nearly all applications of the detector, knowledge of its efficiency (or relative efficiency) characteristics is essential. For detector design purposes it is also of interest to understand how a detector's efficiency is influenced by its size and shape. Since the work of Ewan and Tavendale[1] there have been a number of reports in the literature of efficiency determinations for Ge(Li) detectors.[2]

At present the experimental and the computational approaches to Ge(Li)-detector-efficiency determination require considerable effort to obtain reasonably accurate results. The experimental determination requires that calibrated sources be available throughout the energy range of interest, and that the intensities of the gamma rays be known to a high degree of accuracy. Each separate detector must be individually calibrated for the entire range of energies. The Monte Carlo calculations require considerable computer time. Also, the results obtained are confined to a specific detector.

Described herein is a simplified model of the gamma-ray interaction process that permits relatively rapid and convenient hand calculations of intrinsic total-absorption- and double-escape-peak efficiencies. The simplifications introduced in the model consist in part of parameterizations of some of the functions required in the calculation, in part of averaging certain functions, and in part of making simplifying geometrical assumptions.

In the following section the calculations methods are described. Numerical values and curves are provided to allow the reader to make use of the method if he so wishes. In the next section example results are compared with reported measurements and Monte Carlo calculations. In the final section limitations and possible further applications are discussed.

* Present address: Hewlett-Packard Co., Santa Clara, California.

† This work was supported in part by the U. S. Atomic Energy Commission.

Method

Part I — Total Absorption Peak

Total energy absorption of an incoming gamma-ray photon occurs in a detector when there is either: (1) a photoelectric collision of the incoming photon with an electron or (2) a sequence of Compton collisions terminated by a photoelectric collision. It is assumed here that all scattered electrons are contained in the detector volume. Also, for photons less than 1.5 MeV in energy, pair-production effects can be neglected. The probability of an incoming photon interacting within a detector of depth x is

$$P_{collision} = 1 - e^{-\mu x}, \qquad (1)$$

where $\mu(E)$ is the total linear attenuation coefficient. Of the collisions that do occur, (τ/μ) are photoelectric interactions, and $[1-(\tau/\mu)]$ are Compton interactions. These coefficients, obtained from the tabulation of Chapman,[3] are shown in Fig. 1.

The Compton-scattered photons will undergo further collisions within the sensitive detector volume or escape. The scattered photons that do interact with the detector will themselves be subject to either Compton or photoelectric interactions. Each incoming photon traces a path through the detector volume which ultimately terminates in a photoelectric collision or an escape. The total-absorption probability can be represented by the expression

$$\text{Total-absorption probability} = P_0 + C_0P_1 + C_0C_1P_2 + \cdots + C_0C_1C_2\cdots C_{n-1}P_n + \cdots, \qquad (2)$$

where P_0 = probability that the incoming photon, of energy E_0, undergoes photoelectric collision,

C_0 = probability that the incoming photon undergoes Compton collision,

P_1 = probability that the singly-Compton-scattered photon of reduced energy E_1 has a photoelectric collision,

⋮

C_{n-1} = probability that an (n-1)th-scattered photon of reduced energy E_{n-1} has a Compton collision,

P_n = probability that an (n)th-scattered photon of reduced energy E_n has a photoelectric collision.

The basis of this calculation is to treat each term in the above expression as the product of independent average probabilities. The first probabilities of the collision chain are, from (1),

$$P_0 = (\tau/\mu)(1-e^{-\mu x}) \text{ and } C_0 = (1-\tau/\mu)(1-e^{-\mu x}), \qquad (3)$$

where x is the detector depth. For the

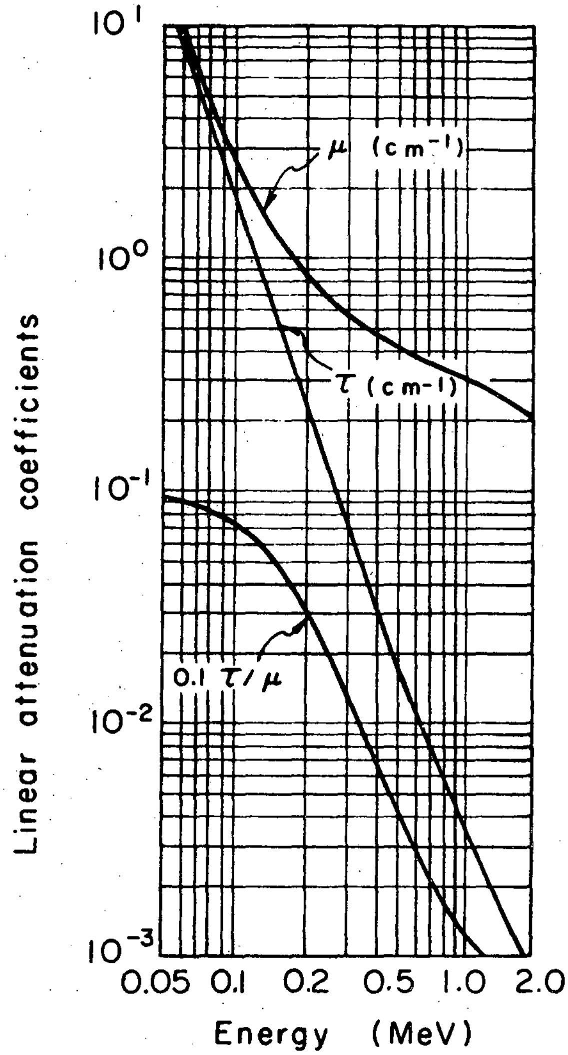

XBL6910- 3968

Fig. 1. Germanium linear attenuation coefficients, showing the total, (μ), photoelectric only, (τ), and the ratio of photoelectric to total (τ/μ). (From Chapman, Ref. 3).

remainder of the P and C probability determinations another approach must be utilized.

The average cross section for a second collision is determined for all Compton-scattered photons resulting from the initial collision of a particular-energy gamma ray, E_0. It can be obtained from the following expression:

$$\bar{\sigma}_t(E_0) = \frac{\int_0^{\pi} \sigma_t[E(\theta, E_0)] \frac{d\sigma}{d\theta}(E_0)\, d\theta}{\sigma_c(E_0)}, \qquad (4)$$

where $\bar{\sigma}_t$ = average total cross section seen by a Compton-scattered photon,

σ_t = total cross section seen by photons of reduced energy E after being scattered into angle θ,

$\frac{d\sigma}{d\theta}$ = differential Compton cross section

for incident photons of energy E_0,
σ_c = total Compton cross section.

Numerical integrations were performed for a number of incident photon energies, using the cross-section values of Nelms.[4] As each σ_t is unique to a particular energy photon, the σ_t's may be used to define the energy of an "average" degraded photon. A plot of average-degraded-photon energy as a function of incident photon energy is given in Fig. 2. The once-scattered photon obtained from this plot can the, in turn, be considered to the incident photon for another collision for which a twice-scattered average-photon energy can be determined. An "average-photon energy-degradation chain" can therefore be established with this curve for any initial gamma-ray photon energy up to 2 MeV.

For the calculation of subsequent collision probabilities we assume each Compton-scattered photon to have a characteristics "average" energy as determined above and, on the average, to originate uniformly throughout the detector volume with an isotropic angular distribution.

The calculation of the probability of a collision, or successive collisions, by averaging methods has received considerable attention in nuclear reactor analysis, particularly with regard to fast-neutron collisions in fuel elements. We have adopted such a method here, the chord method, first used by Dirac.[5] We use the escape probability curves of Dresner,[6] given as a function of "characteristic dimension," $\bar{s}\mu$, where $\bar{s}$ is the average chord length of a volume and μ is the linear attenuation coefficient. The quantity, $\bar{s}$, for a volume with a nonreentrant surface, has the simple form

$$\bar{s} = 4V/A, \tag{5}$$

where V is the volume and A is the total surface area of the body. Thus, the "characteristic dimension," $\bar{s}\mu$, can be determined readily for a specific detector and photon energy. The results of Dresner are given in Fig. 3 for a sphere, an infinite cylinder, and an infinite slab. For the results reported here the sphere data were used.[7]

The steps, then for determining each of the P_n and C_n values of Eq. (2) are as follows:

1) The energy, E_n, of the average nth scattered photon is found from E_{n-1} and Fig. 2 (where E_0 is the energy of the incident photon).

2) For the photon of energy E_n, μ and (τ/μ) are then obtained from Fig. 1.

3) The interaction probability, P_c, is read as a function of $\bar{s}\mu$ from Fig. 3(using the curve labeled "sphere"), where $\bar{s}$ was calculated from Eq. (5).

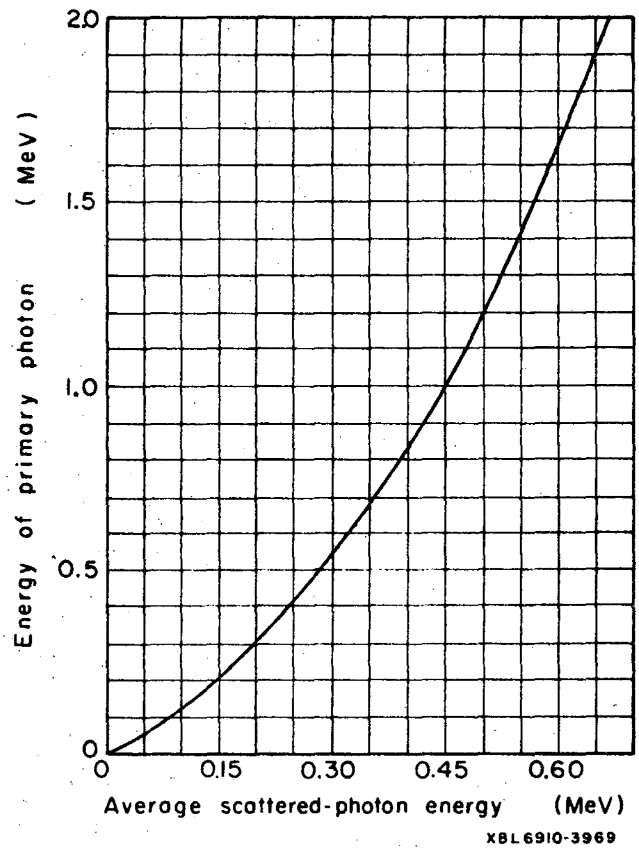

Fig. 2. Average-energy-degradation curve for Ge.

4) Then,

$$P_n = (\tau/\mu)\ P_c,$$
$$C_n = \left[1 - (\tau/\mu)\right] P_c.$$

Finally, the P_n and C_n values are combined in Eq. (2) to give the total absorption probability. The sum [Eq. (2)] typically converges to within 1% of its total value in a maximum of six to seven terms.

Part II — Double-Escape Peak

Double-escape-peak efficiencies are calculated as the product of the probabilities of (a) pair production, (b) total absorption of the electron-positron pair, and (c) complete escape of the positron-annihilation gamma rays. It is assumed in the calculation that these three probabilities can be treated independently.

Thus,

$$P_{dep} = P_{pp} \cdot P_A \cdot P_{de}, \tag{6}$$

where P_{dep} = probability of a double-escape-peak event,

P_{pp} = probability of pair production,

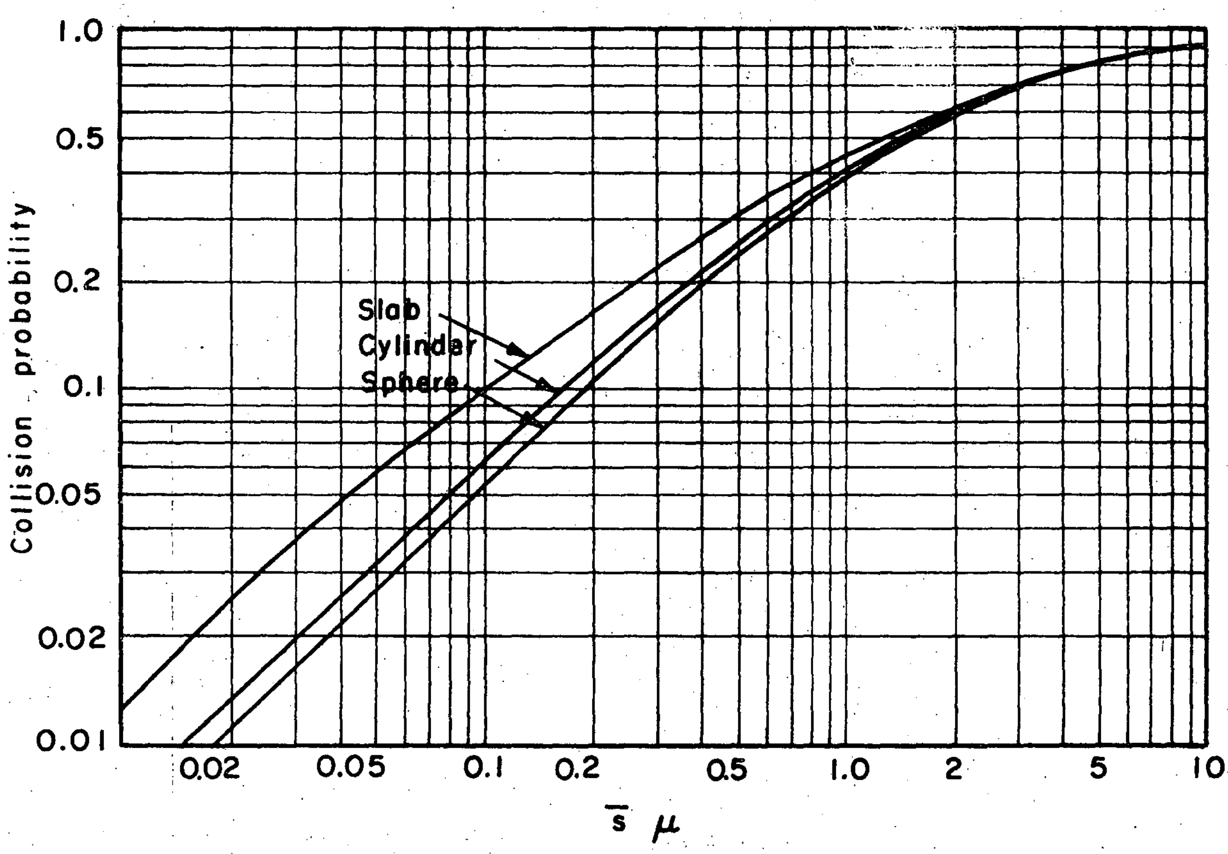

XBL6910-3971

Fig. 3. Collision probability as a function of the characteristic dimension, $\bar{s}\mu$, for a sphere, an infinite cylinder, and an infinite slab. The parameter $\bar{s}$ is the average cord length of a volume and μ is the total linear attenuation coefficient.

P_A = probability for electron-positron absorption,

P_{de} = probability of annihilation photon double escape.

(a) Pair Production

The probability for pair production, P_{pp}, in a detector of thickness x is given by Eq. (1), multiplied by κ/μ

$$P_{pp} = \frac{\kappa}{\mu}\ (1 - e^{-\mu x}), \qquad (7)$$

where κ is the partial attenuation coefficient for a pair-production interaction. The linear attenuation coefficients for germanium in the energy range of interest here are given in Fig. 4.

(b) Electron-Positron Absorption

Whereas the probability of electron escape was neglected in Part I, here, because of the higher electron energies, it is a much more important factor and must be considered in some detail. It is, however, assumed that the electrons are emitted in the forward direction. This simplifies the problem to one-dimensional geometry.

For a photon of energy E_γ, the total energy available to the electron-positron pair is $E_p = E_\gamma - 1.022$ MeV. If the higher energy of the two electrons is E_1 then the probability of total absorption of the pair is

$$P_A(x, E_\gamma) = \int_0^x \int_{E_{p/2}}^{E_p} S(x')P_{Ae}(x'E_1)\ P_{Ae}(x', E_p - E_1)\ P(E_1)\ dx'dE_1, \qquad (8)$$

where $S(x')$ = relative probability of production of particle pairs at x',

$P_{Ae}(x', E)$ = absorption probabilitiy of e^- (or e^+) produced at x' with energy E,

$P(E_1)$ = probability of the higher energy particle having energy E_1,

$P_A(x, E_\gamma)$ = probability of two-particle absorption in detector of width x.

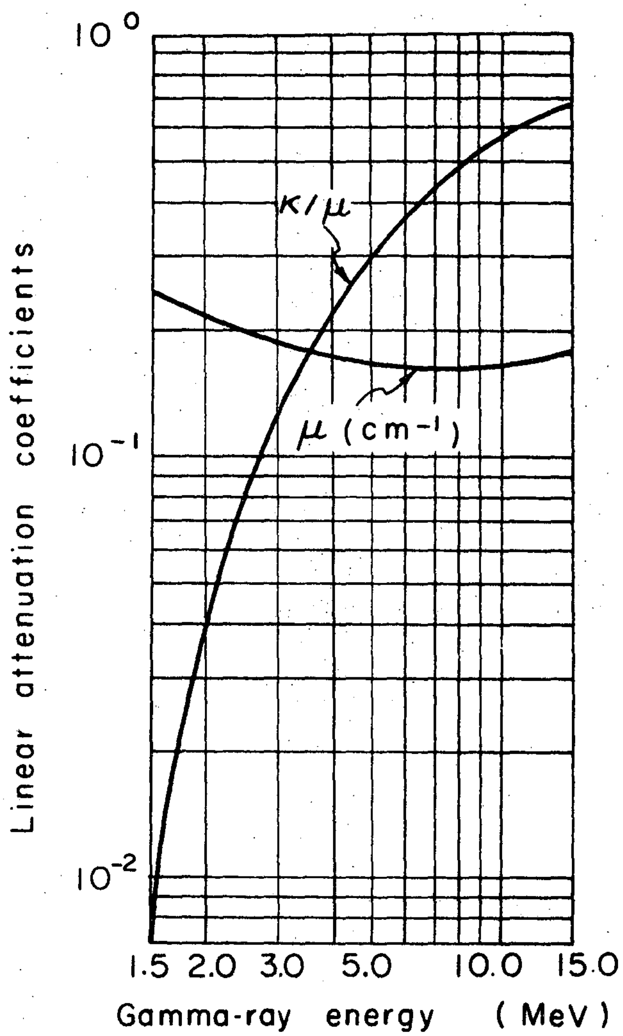

XBL6910-3970

Fig. 4. Germanium linear attenuation coefficients. The curves shown are the total attenuation coefficient (μ) and the ratio of pair-production interactions to total (κ/μ). (From Chapman, Ref. 3).

In the evaluation of this expression the following simplifying approximations are made:[2]

1) Attenuation of the incident gamma-ray beam is neglected. Hence

$$S(x') \equiv 1/x.$$

2) All values of $e^-(e^+)$ energy are assumed equally likely. Hence

$$P(E_1) \equiv 2/E.$$

3) The probability of electron containment, $P_A(x', E)$, was parameterized by using as a guide the electron absorption data of Marshall and Ward[8] and the range relationship given in Siegbahn.[9] The simplified forms used were

$$P_A(x', E) = 0 \qquad x' < 0.24\,R$$

$$= (x' - 0.24\,R)/(0.76\,R) \qquad 0.24\,R \leq x' \leq R,$$

where R, the maximum electron range, was taken to be

$$R = 0.1087E(\text{MeV})$$

The calculated $P_A(x, E_\gamma)$ is shown in Fig. 5 (top curve) as a function of x/R_M, where R_M is $R(E_\gamma - 1.022\text{ MeV})$.

In addition, bremsstrahlung effects were considered. At these energies there is a significant probability that electrons emit bremsstrahlung and that the bremsstrahlung escape.

To parameterize this effect it was assumed that the probability per unit path length of emission of a bremsstrahlung of energy E_B was $P_B = a/E_B$, where a is a constant.

The probability per unit path length that an electron of energy E' will produce a bremsstrahlung of energy greater than ϵ then becomes

$$\int_{\epsilon}^{E'} a/E_B\, dE_B = a \ln E'/\epsilon .$$

If $P_{\bar{B}}(y)$ is defined as the probability that an electron travels a distance y without producting a bremsstrahlung of energy greater than ϵ and it is assumed that the total path length traveled by an electron of energy E is its maximum range, R, then

$$P_{\bar{B}}(R) = \exp\left[-(aR\epsilon/E)(E/\epsilon \ln E/\epsilon - E/\epsilon + 1)\right]. \quad (9)$$

For the results presented here ϵ has been set equal to 0.1 MeV. This means that, for the purposes of these calculations, all bremsstrahlung of lower energy are assumed to be contained by the crystal and all of higher energy are assumed to escape (cf. Fig. 1). The constant, $a = \ell_R^{-1}$ where ℓ_R is the radiation length in Ge, was taken to be $a = 0.423\text{ cm}^{-1}$.[10] When the factors $P_{\bar{B}}[R(E_1)]$ and $P_{\bar{B}}[R(E_p - E_1)]$ [Eq. (9)] are included inside the intergal [Eq. (8)] we obtain, by numerical integration, a $P_A(x, E_\gamma)$ that is explicitly energy dependent. A family of curves for E_γ = 2, 4, 6, 8, and 10 MeV is shown in Fig. 5.

(c) Annihilation-Photon Double Escape

The probability of annihilation-photon double escape, P_{de}, is obtained by using Fig. 3. Whereas previously the parameter of interest was the probability of collision, now the parameter of interest is the probability of complete photon escape from the detector volume. The procedure, then, is to determine the characteristic dimension $\bar{s}\mu$ for the 0.511-MeV photon for the detector studied. With the characteristic dimension, the probability of collision is determined ("sphere" curve). The probability of escape, P_{esc}, is

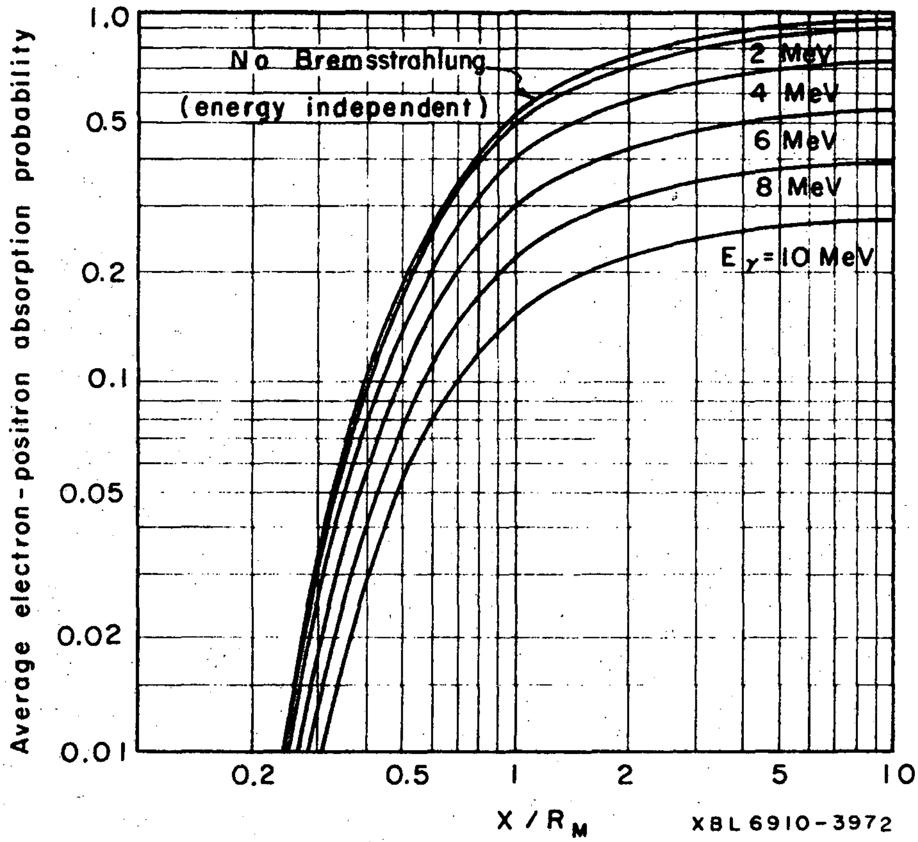

Fig. 5. Average electron-positron energy absorption probabilities as a function of the ratio of detector depth to maximum electron range (x/R_M). In the top curve the effect of bremsstrahlung is not included and the results are energy independent.

$$P_{esc} = 1 - P_c .$$

The probability of double escape then is

$$P_{de} = P_{esc}^{\ 2} = (1-P_c)^2 .$$

To review: the steps for determining the double-escape-peak efficiency for a gamma ray of energy E_γ are:

1) For E_γ, find μ and κ/μ (Fig. 4) and calculate P_{pp} [Eq. (7)].

2) Evaluate $x/R_M = x/[0.1087(E_\gamma - 1.022)]$ and obtain P_A from Fig. 5.

3) Evaluate $\bar{s}\mu$ ($\mu_{0.511\ \mathrm{MeV}} = 0.42\ \mathrm{cm}^{-1}$), obtain P_c from Fig. 3, and evaluate $P_{de} = (1-P_c)^2$.

4) The efficiency is then determined as the product of the above three results [Eq. (6)].

Results

Figure 6 presents a comparison of the intrinsic total-absorption-peak-efficiency values of two planar Ge(Li) detectors of the same reported cross section area (2.5 cm^2) but of slightly different reported thickness (3.5 mm vs. 4.0 mm). The upper data points (Ewan and Tavendale[1]) and the lower experimental curve of Cline,[11] (d), are compared with (a) Monte Carlo calculations of Wainio and Knoll,[12] (b) Monte Carlo calculations of de Castro Faria and Levesque,[13] and (c) results of this paper. In both cases the curve shapes calculated by the method given here agree quite well with experiment. Although the Monte Carlo calculations fit the upper data more closely, ours fit more closely to the lower, both in value and in shape. In both cases the differences between the efficiences calculated here and the experimental measurements are less than, or on the order of, 0.5 mm detector-thickness equivalent.

In Figure 7 calculations are compared with reported measurements on three larger detectors. The upper set of data (d) shows the experimental curve of Cline[11] (the reported area of his detector was actually 4.9 cm^2) and two data points of Ewan and Tavendale.[1] The lower set of data points is from Michaelis.[14] The authorship of the calculated curves is indicated by the same letter symbols used in Fig. 6. The X's on curve (a) show the energy values at which the Monte Carlo calculations were made. Again the curve shapes calculated here agree quite well with

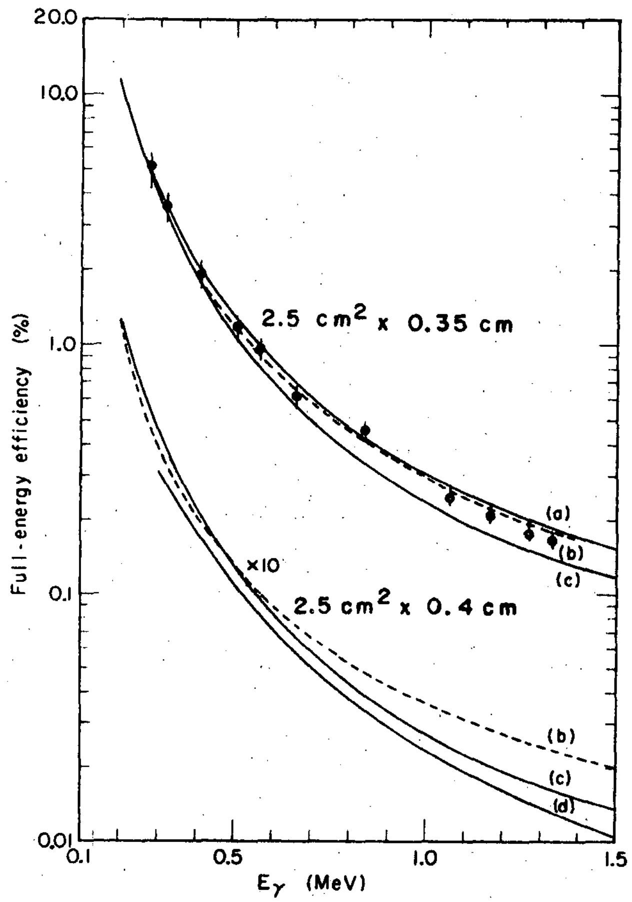

XBL6910-6038

Fig. 6. Total-absorption-peak efficiencies for two detectors, each of cross-section area 2.5cm^2. The experimental measurements of Ewan and Tavendale (Ref. 1) are shown as data points. The curves represent the following:
(a) the Monte Carlo calculations of Wainio and Knoll (Ref. 12).
(b) the Monte Carlo calculations of de Castro Faria and Levesque (Ref. 13).
(c) the present calculations.
(d) the experimental measurements of Cline (Ref. 11).

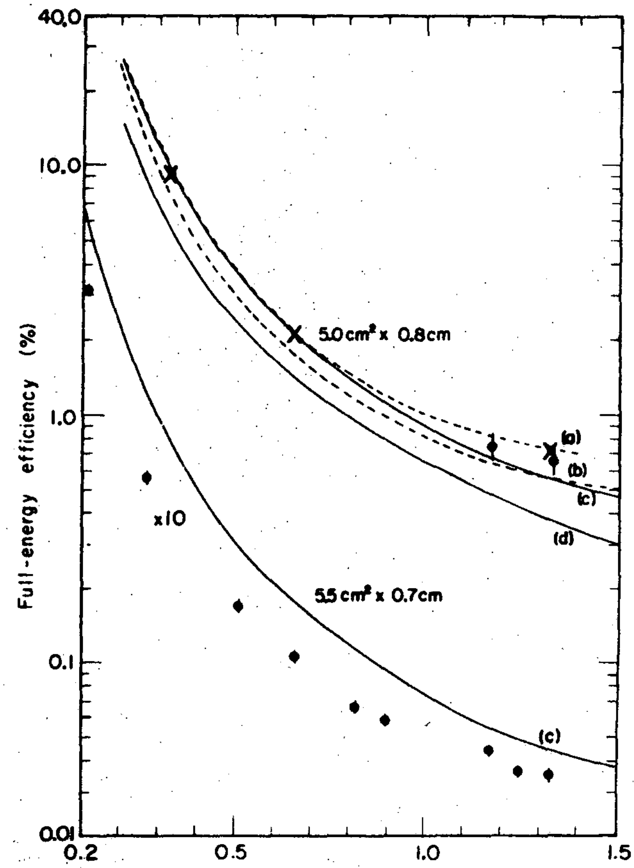

Fig. 7. Total-absorption-peak efficiencies for two detectors. The experimental measurements of Ewan and Tavendale (Ref. 1) are shown as data points in the upper group of curves, while the measurements of Michaelis (Ref. 14) are shown beneath the lower curve. The Monte Carlo-calculated efficiency values of Wainio and Knoll (Ref. 12) are indicated by crosses, ×. The curves represent the following:
(a) the Monte Carlo calculation of Wainio and Knoll (Ref. 12).
(b) the Monte-Carlo calculations of de Castro Faria and Levesque (Ref. 13).
(c) the present calculations.
(d) the experimental measurements of Cline (Ref. 11).

experiment; however, the absolute values calculated are in somewhat greater disagreement than for the smaller detectors (Fig. 6). It should be pointed out, though, that in the upper set of data the reported experimental results for two detectors of the same thickness and cross-section area differ from each other by an even larger amount, and the calculated curve of this work lies between them.

Figure 8 presents a comparison of intrinsic double-escape-peak-efficiency values of a 2.5 cm^2 × 0.35 cm planar Ge(Li) detector. The data points are those of Wean and Tavendale.[1] Curves (a) and (b) are the Monte Carlo-calculated results of de Castro Faria and Levesque[13] and Wainio and Knoll,[12] respectively. Curve (c) presents the results obtained by the method of this work.

Figure 9 presents further comparisons of the results of this work [curve (b)] with the calculated results of de Castro Faria and Levesque[13] and the experimental-measurement results of Cline.[11] Monte Carlo-calculated data points of Wainio and Knoll[12] are indicated as circles, O.

The results of the method of this work more closely resemble the Monte Carlo-calculated results of Wainio and Knoll[12] (this agreement is

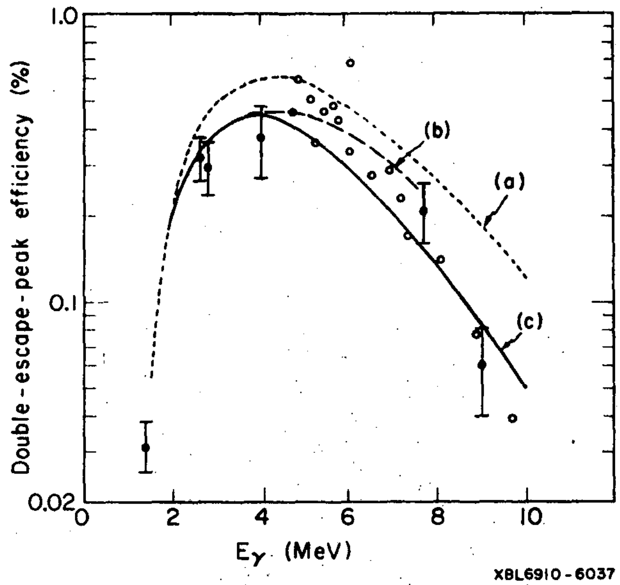

Fig. 8. Double-escape-peak efficiencies for a 2.5 $cm^2 \times 0.35$ cm detector. The experimental measurements of Ewan and Tavendale (Ref. 1) are shown as data points. The curves represent the following:

(a) the Monte Carlo calculations of de Castro Faria and Levesque (Ref. 13).

(b) the Monte Carlo calculations of Wainio and Knoll (Ref. 12).

(c) the present calculations.

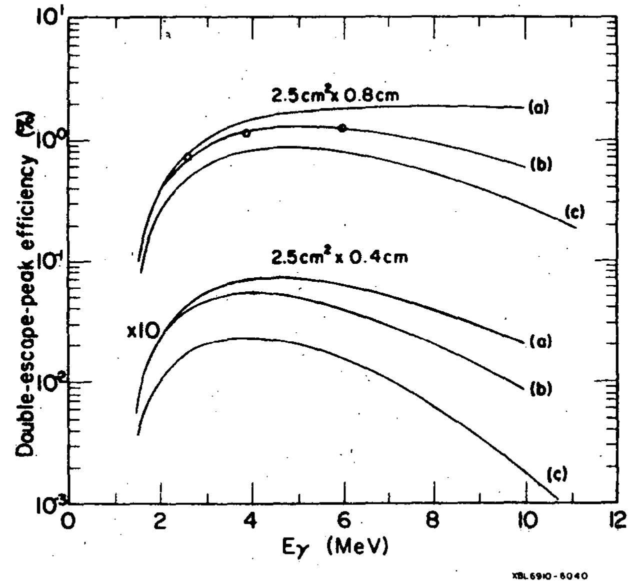

Fig. 9. Double-escape-peak efficiencies for two detectors. The Monte Carlo calculations of Wainio and Knoll (Ref. 12). for a 2.5 $cm^2 \times 0.8$ cm detector are shown as circles, O. The curves represent the following:

(a) the Monte Carlo calculations of de Castro Faria and Levesque (Ref. 13).

(b) the present calculations.

(c) the experimental measurements of Cline, (Ref. 11).

remarkable in Fig. 9), who considered bremsstrahlung effects in their calculation, than the results of de Castro Faria and Levesque,[13] who did not. The present hand-calculation technique gave results very close to the measured values of Ewan and Tavendale,[1] but higher than the measured values of Cline[11] for a pair of detectors not too different in size.

In order to ease the calculational effort in the further application of this method to testing the effects of various parameter adjustments, a computer program has been written that will calculate and plot efficiencies in the manner described here. The results for a sample family of detectors are shown in Figs. 10, 11, and 12. Figures 11 and 12 show double-escape results with and without consideration of bremsstrahlung effects.

Discussions and Conclusions

The semianalytical approximation method described here produces results in good agreement both with Monte Carlo calculations and experiment. Differences from Monte Carlo calculations are comparable to the differences between two Monte Carlo calculations. Furthermore, the method reliably reproduces the shape of measured Ge(Li) efficiency curves. Where differences exist between calculation and measurement they are almost proportional over the entire range of energies considered.

Absolute-value disagreements with experiment may be related to certain approximations. How-

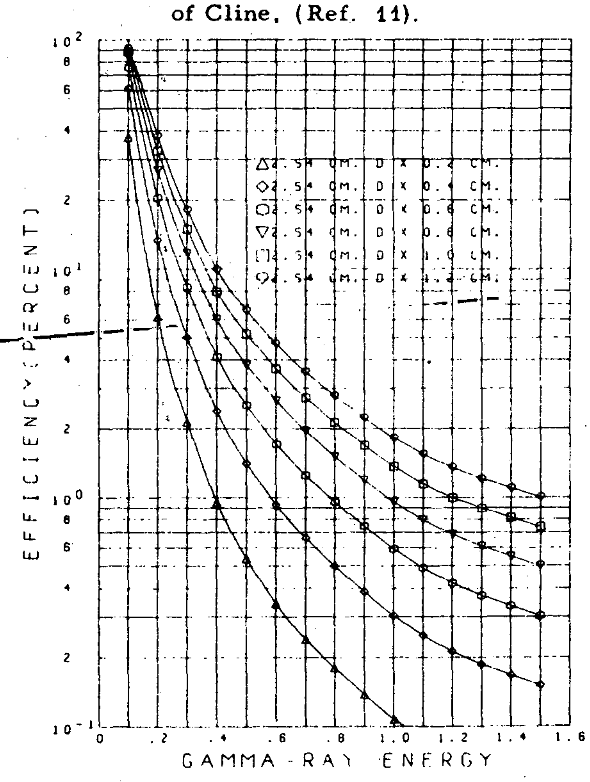

Fig. 10. Calculated Ge(Li) intrinsic full-energy-peak efficiencies for a family of cylindrical planar detectors.

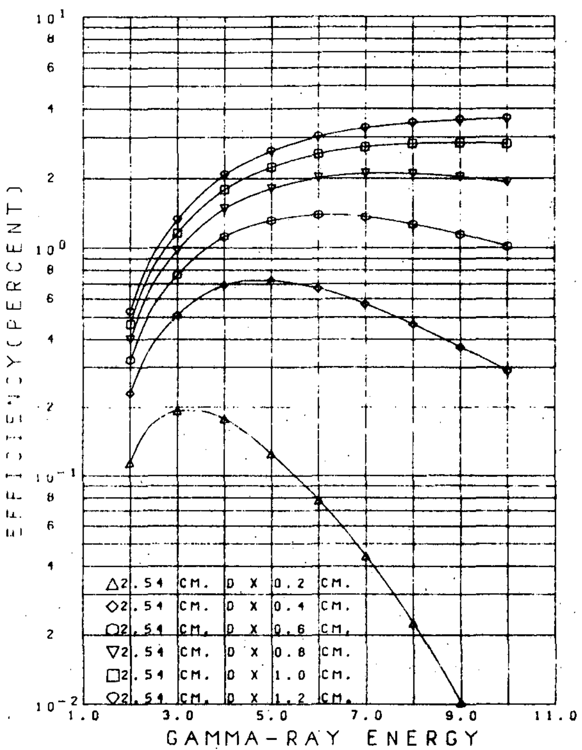

XBL 6910-5854

Fig. 11. Calculated Ge(Li) intrinsic double-escape-peak efficiencies for a family of cylindrical planar detectors. Losses due to bremsstrahlung are neglected.

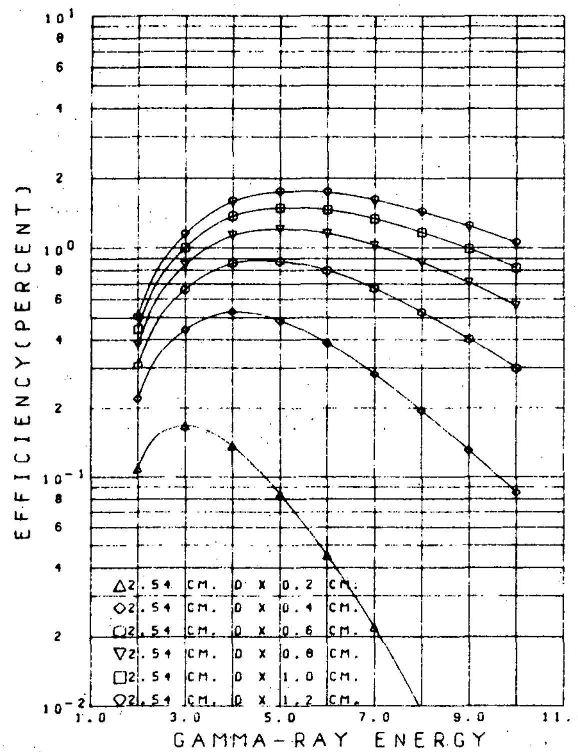

XBL 6910-5852

Fig. 12. Calculated Ge(Li) intrinsic double-escape efficiencies for a family of cylindrical planar detectors. Losses due to bremsstrahlung are included.

ever, on the average the Monte Carlo disagreement with experiment is even greater. Other possible sources of this disagreement lie in the interpretation of experimental data. The calculation assumes a parallel beam uniformly illuminating the front surface of the detector and that the detector is sensitive at its surface and over the entire reported volume. Nonparallel incidence, a surface dead layer, and a somewhat reduced sensitive volume can each contribute to disagreement between experiment and calculation. [A slight correction was included here for the 0.5-mm dead layer reported by Michaelis (Fig. 7); the correction was observable only at energies below 0.2 MeV]. The true sensitive dimensions of a detector are not easily determined. This question is considered in some detail by Walford and Doust.[15]

At present the method is applicable only to materials with nonreentrant surfaces. Therefore, excluded from the present analysis are five-sided and coaxial detectors. However, it is hoped that with some modification the method will eventually lend itself to this analysis also. In addition, it should be pointed out that for detectors with dimensions comparable to gamma-ray collision mean free paths, one of the assumptions, that of uniform volume distribution of secondary sources, is no longer valid. Hence, calculations using the methods described here are expected to be less applicable for very large detectors.

In summary, the methods developed here should considerably ease the fairly precise determination of theoretical efficiencies for detectors of various sizes and shapes. It is further hoped that the use of the technique will lead to greater qualitative understanding of the relative importance of various aspects of photon-energy containment by gamma-ray detectors. The Dirac chord method should prove especially useful for photon detection and attenuation problems.

Acknowledgments

The authors would like to express their gratitude to Mr. Robert New who was instrumental in adapting these calculations to computer processing. We would also like to thank Mr. Gary Born who performed the bremsstrahlung calculations.

REFERENCES

1. G. T. Ewan and A. J. Tavendale, Can. J. Phys. 42, 2286 (1964).
2. For a detailed bibliography, see B. Euler, M.S. thesis, University of California, Berkeley, 1969. Also presented here is a more detailed description of the development of most of the approximations used in these calculations.
3. G. T. Chapman, Nucl. Instr. Methods 52, 101 (1967).
4. A. T. Nelms, Graphs of the Compton Energy-

Angle Relationship and the Klein-Nishina Formula from 10 keV to 500 MeV (National Bureau of Standards Circular 542, U.S. Government Printing Office, Washington 25, D. C.).

5. P. A. M. Dirac, Approximate Rate of Neutron Multiplication for a Solid of Arbitrary Shape and Uniform Density, British Report M.S.D. 5, Part I. General Theory, 1943.
6. L. Dresner, Resonance Absorption in Nuclear Reactors (Interational Series of Monographs on Nuclear Energy, Vol. 4, Pergamon Press, 1960), p. 65. The Dresner escape probability curves are also presented in R. V. Meghreblian and D. K. Holmes, Reactor Analysis, (McGraw-Hill Book Company, Inc. New York, 1960), p. 671.
7. The sphere curve is clearly the most appropriate for collision calculations related to Ge(Li) detectors. The infinite cylinder and infinite slab values apply to materials where respectively one or two dimensions are long compared with a collision mean free path—a situation that does not apply here.
8. J. Marshall and A. G. Ward, Can. J. Research A15, 39, (1937).
9. G. Knop and W. Paul, Interaction of Electrons and α-Particles with Matter, in Alpha-, Beta-, Gamma-Ray Spectroscopy, Vol. 1, ed. by K. Siegbahn (North-Holland Publishing Co., Amsterdam, 1965), p. 21.
10. This value was calculated directly from the expression given in J. Orear, A. H Rosenfeld, and R. A. Schluter, Nuclear Physics, a course given by Enrico Fermi (University of Chicago Press, 1949), p. 49.
11. J. E. Cline, IEEE Trans. Nucl. Sci. NS-15, No. 3, 198 (1968).
12. K. M. Wainio and G. F. Knoll, Nucl. Instr. Methods 44, 213 (1966).
13. N. V. de Castro Faria and R. J. A. Levesque, Nucl. Instr. Methods 46, 325 (1967).
14. W. Michaelis, Nucl. Instr. Methods 70, 253 (1969).
15. G. V. Walford and C. E. Doust, Nucl. Instr. Methods 67, 272 (1969).

TECHNICAL INFORMATION DIVISION
LAWRENCE RADIATION LABORATORY
UNIVERSITY OF CALIFORNIA
BERKELEY, CALIFORNIA 94720